Distorted-wave calculations of the electron-impact excitation-autoionization processed from the ground state of highly ionized Ga I–like ions through $\Delta n = 1$ inner-shell excitations

J. Oreg* and W. Goldstein
Lawrence Livermore National Laboratory, P.O. Box 808, Livermore, California 94550

P. Mandelbaum, D. Mitnik, E. Meroz, and J. L. Schwob
Racah Institute of Physics, The Hebrew University, 91904 Jerusalem, Israel

A. Bar Shalom*
Department of Physics and Space Science Laboratory, University of California, Berkeley, California 94720
(Received 5 December 1990)

A systematic investigation of ionization enhancement due to collisional excitation followed by autoionization (EA) is presented for Ga I–like rare-earth elements. Both nuclear charge and temperature dependence are analyzed and compared with direct-impact ionization (DI) rates. Collisional excitation and autoionization rates were calculated in the distorted-wave factorization-interpolation method. DI rates were calculated by a modified plane-wave Born approximation method. The rates for the combined EA process for selected Ga I–like ions from Mo XII to Dy XXXVI are presented for the relevant temperature ranges. It is shown that indirect ionization is dominant for Mo through Pr but is reduced gradually with Z and approaches zero at Dy. A density diagnosis is provided by the opening of EA channels that are not active at low densities.

I. INTRODUCTION

In low-density plasmas, the relative abundances of atoms in different ionization stages depends on various ionization and recombination rates of the involved ions. It was early suggested by Allen and Dupree [1] that an alternative process to the direct ionization by electron impact that could be of importance in highly ionized atoms is the electron-impact excitation of an inner-shell electron to a bound state lying above the first ionization limit, followed by autoionization.

This process has been studied extensively in the Na I–like sequence by different authors and updated distorted wave calculation for some ions of this sequence can be found in Ref. [2]. In this sequence the ratio of excitation-autoionization to direct ionization rates at a temperature corresponding to half the ionization potential of the ion is found to be from 1.5 to 2. For other neighboring isoelectronic sequences this ratio should be smaller. Indeed, the direct ionization rate increases with the number of external electrons.

However, Cowan and Mann [3] suggested that Cu I–, Zn I–, and Ga I–like ions could be potential candidates for high excitation-autoionization rates. To our best knowledge, no quantitative calculation has ever been performed for these isoelectronic sequences except those presented in a previous work [4], where it has been shown that, indeed, in the Ga I–like praseodymium the rate for excitation-autoionization through $\Delta n = 1$ inner-shell excitations was about four times the direct ionization rate at a temperature of maximum abundance at coronal equilibrium. This could explain the abnormal intensity behavior of Ga I–like lines emitted from rare-earth elements injected in a tokamak plasma.

In the present work, the detailed theoretical results of calculations of excitation-autoionization rates for a selection of Ga I–like ions from Mo XII to Dy XXXVI are given. The case of highly ionized rare-earth elements of the Ga I–like sequence is especially interesting since most of the inner subshell excited levels $3d^9 4s^2 4p 4d, 4f$ lie above the first ionization limit on one hand, and on the other hand there are only three easily removable electrons in the $n = 4$ shell to contribute significantly at intermediate temperature to direct ionization, whereas there are ten $3d$ electron candidates to inner-shell excitation plus autionization.

Details of the theoretical calculation method are given in Sec. II. Section III follows with the results. Section III A presents the calculations along the isoelectronic sequence. In this section the isoelectronic trends and, in particular, the dependence of the ratio of excitation-autoionization (EA) to direct ionization as a function Z are analyzed. The typical temperature dependence is described in Sec. III B. In Sec. IV a density diagnosis provided by the EA process is discussed.

II. THEORY

A. Direct-impact ionization

The rate coefficients for direct-impact ionization (DI) were calculated by a modified plane-wave Born approximation (PWBA) method, using the free-electron approximation suggested by Vainshtein, Presnyakov, and Sobelman [5]. A general tendency of the cross sections calculated by first-order approximation methods is to overestimate the cross section near the threshold. This is due to the fact that these methods usually improve the atomic

 ©1991 The American Physical Society

potential sensed by the incoming electron, and do not take into account the influence of the incoming electron on the wave functions of the atomic electrons. Higher-order approximations are usually prohibitively lengthy for the calculation of rate coefficients. The idea behind this approximation is to improve the description of the interaction between the incoming electron and the ejected electron. This interaction is described initially as a scattering process between free electrons, while the atomic potential appears as a perturbation. A complete description of the approximation can be found in Ref. [5]. The result is obtained by multiplying the differential cross section in the PWBA:

$$\frac{d\sigma_{01}}{d\varepsilon}=\frac{8\pi}{k_0^2}\int_{k_0-k_1}^{k_0+k_1}q^{-3}dq\,|\langle 1|e^{iq\cdot r}|0\rangle|^2 \tag{1}$$

by the factor

$$f(v,x)=\frac{\pi v}{\sinh(\pi v)}F(-iv,iv,1,x),$$

$$v=k_0^{-1},\quad x=\left[\frac{\Delta\varepsilon+q^2}{\Delta\varepsilon+3q^2}\right]^2, \tag{2}$$

giving

$$\frac{d\sigma_{01}}{d\varepsilon}=\frac{8\pi}{k_0^2}\int_{k_0-k_1}^{k_0+k_1}q^{-3}dq\,|\langle 1|e^{iq\cdot r}|0\rangle|^2[f(v,x)]^2, \tag{3}$$

where ε is the energy of the ejected electron, k_0 the momentum of the incoming electron, $q=k_0-k_1$ the momentum transfer, $\Delta\varepsilon=k_0^2-k_1^2$, and F is the hypergeometric function. Results using this method were formerly published for hydrogen ionization cross sections. Here this approximation has been used for multielectron ions of the Ga I–like isoelectronic sequence, and in this implementation the atomic potential in the central field approximation was calculated using the RELAC code [6]. The method was tested in many other cases and results were found to be practically identical to those found by use of much more complicated methods (Coulomb Born, distorted wave). A marked improvement near the threshold has been observed, whereas the results far from threshold coincide with those of the PWBA, as $f(v,x)$ tends to unity for k_0^2 much bigger than $\Delta\varepsilon$.

B. Excitation autoionization rates

In the isolated-resonance approximation the excitation-autoionization (EA) rate from an initial level i of the Ga I–like $3d^{10}4s^24p$ configuration to a level k of the Zn I–like $3d^{10}4s^2$ or $3d^{10}4s4p$ configuration is given by

$$X_{ik}\equiv\sum_j Q_{ij}\left[\frac{A^a_{jk}}{\sum_l A^a_{jl}+\sum_m A_{jm}}\right], \tag{4}$$

where Q_{ij} is the electron impact excitation rate from level i to level j of the intermediate Ga I–like highly excited $3d^94s^24p4d$ or $3d^94s^24p4f$ configurations. A^a_{jk} is the autoionization rate from level j to level k (of the Zn I–like ion). A_{jm} are the radiative decay rates from the inner-shell excited levels to low-lying m levels of the Ga I–like ion. We have included decays to all the low-lying configurations $3d^{10}4s^24p,4d,4f$. Three hundred levels of the Ga I–like ions and 14 levels of the Zn I–like ions were included in the present detailed model which also account for configuration mixing between $3d^94s^24p4f$ and $3d^94s^24d^2$ configurations. The contribution to EA from excitation to $3d^94s^24p5f$ was also calculated but results have shown that it could be neglected.

For the collisional rates, Q_{ij} computations, the factorization method [7] was used. Level energies, ionization potentials (χ's), and radiative transition rates were obtained by the RELAC code. The distorted-wave autoionization rates from an inner-shell excited state ψ'' into all the states ψ of a given level of the neighboring ion are given by the matrix elements

$$A^{\psi''}_{\psi}=\sum_{\tilde{j}}\sum_{j_T,M_T}\left|\left\langle\psi(\Gamma,J)\tilde{j}J_TM_T\left|\sum_{i<j}(e/r_{ij})\right|\psi''(\Gamma'',J''_T,M''_T)\right\rangle\right|^2, \tag{5}$$

where the outer sum is over continuum orbitals $\tilde{j}\equiv(E_{\tilde{j}},l_{\tilde{j}},\tilde{j})$, and the inner sum is over all angular momentum coupling of the target and the continuum electron. Note that by conservation of angular momentum only one term contributes to the sum over J_T,M_T in Eq. (5).

These matrix elements were calculated using a newly developed code [8] based on the relativistic parametric potential method [6]. In these calculations, the same atomic potential, obtained by the variational method, was used for the bound and continuum electrons. The method has been tested and found in very good agreement with the multiconfiguration Dirac-Fock method [8].

III. RESULTS: COMPARISON BETWEEN THE EA AND THE DI PROCESSES

A. Z dependence

In Tables I(a)–I(e), results of the computations for direct ionization of $4p,4s$ and $3d$ electrons as well as for EA are given for a temperature ranging from 0.3χ to 2χ, for various elements from Mo ($Z=42$) to Dy ($Z=66$). These results are given separately for each of the two initial levels $3d^{10}4s^24p_{1/2,3/2}$ of the Ga I–like ion and each of the final levels of the Zn I–like ion. Summation has been performed on all inner-shell excited autoionizing levels of the Ga I–like ion which can be excited from the

TABLE I. Excitation-autoionization rates through $\Delta n = 1$ inner-shell excitations compared to direct ionization rates for selected ions of the Ga I–like isoelectronic sequence for (a) Mo^{11+}, (b) Ag^{16+}, (c) Xe^{23+}, (d) Pr^{28+}, (e) Eu^{32+}, and (f) Dy^{35+}. The rates have been calculated in the electronic temperature range from 0.3 to 2 times the first ionization potential energy (χ). The rates are given in the form $0.XX[-YY]$ which means $0.XX \times 10^{-YY}$ cm^3 sec^{-1}.

(a) Mo^{11+} (χ=226 eV)

	T_e/χ	0.3	0.4	0.5	0.6	0.7	0.8	1.0	1.2	1.6	2.0
Direct ionization											
$4p$		0.12[−10]	0.33[−10]	0.58[−10]	0.89[−10]	0.12[−9]	0.15[−9]	0.20[−9]	0.25[−9]	0.34[−9]	0.40[−9]
$4s$		0.12[−10]	0.35[−10]	0.66[−10]	0.10[−9]	0.14[−9]	0.18[−9]	0.25[−9]	0.32[−9]	0.43[−9]	0.51[−9]
$3d$		0.67[−12]	0.46[−11]	0.15[−10]	0.36[1−10]	0.64[−10]	0.11[−9]	0.21[−9]	0.32[−9]	0.59[−9]	0.88[−9]
Total rate		0.25[−10]	0.73[−10]	0.14[−9]	0.23[−9]	0.33[−9]	0.44[−9]	0.66[−9]	0.89[−9]	0.14[−8]	0.18[−8]
Excitation-autoionization process											
From $4p_{1/2}$ to $3d^{10}4s^2$		0.25[−10]	0.62[−10]	0.10[−9]	0.14[−9]	0.18[−9]	0.22[−9]	0.27[−9]	0.31[−9]	0.36[−9]	0.38[−9]
$4s4p_{1/2}$	$[J=0]$	0.12[−10]	0.29[−10]	0.49[−10]	0.68[−10]	0.87[−10]	0.10[−9]	0.13[−9]	0.15[−9]	0.17[−9]	0.19[−9]
$4s4p_{1/2}$	$[J=1]$	0.32[−10]	0.79[−10]	0.13[−9]	0.19[−9]	0.24[−9]	0.28[−9]	0.36[−9]	0.41[−9]	0.48[−9]	0.52[−9]
$4s4p_{3/2}$	$[J=1]$	0.96[−11]	0.24[−10]	0.41[−10]	0.58[−10]	0.75[−10]	0.89[−10]	0.11[−9]	0.13[−9]	0.16[−9]	0.17[−9]
$4s4p_{3/2}$	$[J=2]$	0.83[−11]	0.20[−10]	0.33[−10]	0.46[−10]	0.58[−10]	0.68[−10]	0.84[−10]	0.95[−10]	0.11[−9]	0.11[−9]
$4s4d_{3/2}$	$[J=1]$	0.17[−11]	0.48[−11]	0.87[−11]	0.13[−10]	0.17[−10]	0.20[−10]	0.27[−10]	0.31[−10]	0.37[−10]	0.41[−10]
$4s4d_{3/2}$	$[J=2]$	0.22[−11]	0.63[−11]	0.11[−10]	0.17[−10]	0.22[−10]	0.28[−10]	0.36[−10]	0.43[−10]	0.53[−10]	0.59[−10]
$4s4d_{5/2}$	$[J=3]$	0.19[−11]	0.53[−11]	0.97[−11]	0.14[−10]	0.19[−10]	0.23[−10]	0.30[−10]	0.36[−10]	0.43[−10]	0.48[−10]
$4s4d_{5/2}$	$[J=2]$	0.18[−11]	0.51[−11]	0.93[−11]	0.14[−10]	0.18[−10]	0.22[−10]	0.29[−10]	0.34[−10]	0.41[−10]	0.45[−10]
Total via $3d^9 4s^2 4p4d$		0.65[−10]	0.15[−9]	0.25[−9]	0.34[−9]	0.41[−9]	0.48[−9]	0.58[−9]	0.64[−9]	0.71[−9]	0.73[−9]
Total via $3d^9 4s^2 4p4f$		0.30[−10]	0.85[−10]	0.15[−9]	0.23[−9]	0.31[−9]	0.38[−9]	0.51[−9]	0.61[−9]	0.75[−9]	0.86[−9]
Total rate[a]		0.95[−10]	0.24[−9]	0.40[−9]	0.57[−9]	0.72[−9]	0.86[−9]	0.11[−8]	0.13[−8]	0.15[−8]	0.16[−8]
From $4p_{3/2}$ to $3d^{10}4s^2$		0.15[−10]	0.39[−10]	0.67[−10]	0.95[−10]	0.12[−9]	0.15[−9]	0.19[−9]	0.22[−9]	0.26[−9]	0.28[−9]
$4s4p_{1/2}$	$[J=0]$	0.18[−11]	0.45[−11]	0.76[−11]	0.11[−10]	0.14[−10]	0.16[−10]	0.20[−10]	0.23[−10]	0.27[−10]	0.29[−10]
$4s4p_{1/2}$	$[J=1]$	0.12[−10]	0.30[−10]	0.50[−10]	0.69[−10]	0.86[−10]	0.10[−9]	0.13[−9]	0.14[−9]	0.16[−9]	0.17[−9]
$4s4p_{3/2}$	$[J=2]$	0.42[−10]	0.10[−9]	0.17[−9]	0.23[−9]	0.29[−9]	0.35[−9]	0.43[−9]	0.49[−9]	0.57[−9]	0.60[−9]
$4s4p_{3/2}$	$[J=1]$	0.14[−10]	0.33[−10]	0.56[−10]	0.78[−10]	0.99[−10]	0.12[−9]	0.15[−9]	0.17[−9]	0.20[−9]	0.21[−9]
$4s4d_{3/2}$	$[J=1]$	0.15[−11]	0.40[−11]	0.72[−11]	0.11[−10]	0.14[−10]	0.17[−10]	0.22[−10]	0.25[−10]	0.30[−10]	0.33[−10]
$4s4d_{3/2}$	$[J=2]$	0.31[−11]	0.88[−11]	0.16[−10]	0.24[−10]	0.32[−10]	0.40[−10]	0.53[−10]	0.64[−10]	0.79[−10]	0.89[−10]
$4s4d_{5/2}$	$[J=3]$	0.32[−11]	0.91[−11]	0.17[−10]	0.25[−10]	0.33[−10]	0.41[−10]	0.55[−10]	0.66[−10]	0.81[−10]	0.92[−10]
$4s4d_{5/2}$	$[J=2]$	0.22[−11]	0.61[−11]	0.11[−10]	0.17[−10]	0.22[−10]	0.27[−10]	0.36[−10]	0.43[−10]	0.53[−10]	0.59[−10]
Total via $3d^9 4s^2 4p4d$		0.65[−10]	0.15[−9]	0.25[−9]	0.34[−9]	0.41[−9]	0.48[−9]	0.57[−9]	0.64[−9]	0.73[−9]	0.73[−9]
Total via $3d^9 4s^2 4p4f$		0.30[−10]	0.85[−10]	0.15[−9]	0.23[−9]	0.31[−9]	0.38[−9]	0.51[−9]	0.61[−9]	0.76[−9]	0.86[−9]
Total rate[a]		0.95[−10]	0.24[−9]	0.40[−9]	0.57[−9]	0.72[−9]	0.86[−9]	0.11[−8]	0.13[−8]	0.15[−8]	0.16[−8]

(b) Ag^{16+} (χ=400 eV)

	T_e/χ	0.3	0.4	0.5	0.6	0.7	0.8	1.0	1.2	1.6	2.0
Direct ionization											
$4p$		0.49[−11]	0.13[−10]	0.23[−10]	0.35[−10]	0.46[−10]	0.58[−10]	0.80[−10]	0.98[−10]	0.13[−9]	0.15[−9]
$4s$		0.55[−11]	0.16[−10]	0.32[−10]	0.45[−10]	0.62[−10]	0.80[−10]	0.11[−9]	0.14[−9]	0.18[−9]	0.22[−9]
$3d$		0.38[−12]	0.24[−11]	0.76[−11]	0.18[−10]	0.30[−10]	0.50[−10]	0.91[−10]	0.14[−9]	0.27[−9]	0.38[−9]
Total rate		0.11[−10]	0.31[−10]	0.63[−10]	0.98[−10]	0.15[−9]	0.19[−9]	0.28[−9]	0.39[−9]	0.58[−9]	0.75[−9]

TABLE I. (*Continued*).

(b) Ag^{16+} (χ=400 eV)

	T_e/χ	0.3	0.4	0.5	0.6	0.7	0.8	1.0	1.2	1.6	2.0
Excitation-autoionization process											
From $4p_{1/2}$ to $3d^{10}4s^2$		0.51[−10]	0.11[−9]	0.18[−9]	0.24[−9]	0.29[−9]	0.33[−9]	0.40[−9]	0.44[−9]	0.49[−9]	0.52[−9]
$4s4p_{1/2}$	[J=0]	0.91[−11]	0.21[−10]	0.35[−10]	0.48[−10]	0.59[−10]	0.69[−10]	0.84[−10]	0.95[−10]	0.11[−9]	0.12[−9]
$4s4p_{1/2}$	[J=1]	0.18[−10]	0.44[−10]	0.74[−10]	0.10[−9]	0.13[−9]	0.16[−9]	0.19[−9]	0.22[−9]	0.26[−9]	0.29[−9]
$4s4p_{3/2}$	[J=1]	0.47[−11]	0.12[−10]	0.20[−20]	0.29[−10]	0.36[−10]	0.43[−10]	0.54[−10]	0.63[−10]	0.74[−10]	0.83[−10]
$4s4p_{3/2}$	[J=2]	0.41[−11]	0.99[−11]	0.17[−10]	0.23[−10]	0.29[−10]	0.34[−10]	0.42[−10]	0.48[−10]	0.55[−10]	0.61[−10]
Total via $3d^9 4s^2 4p4d$		0.48[−10]	0.10[−9]	0.16[−9]	0.21[−9]	0.25[−9]	0.28[−9]	0.33[−9]	0.36[−9]	0.39[−9]	0.39[−9]
Total via $3d^9 4s^2 4p4f$		0.40[−10]	0.10[−9]	0.17[−9]	0.24[−9]	0.31[−9]	0.37[−9]	0.46[−9]	0.53[−9]	0.63[−9]	0.71[−9]
Total rate[a]		0.88[−10]	0.20[−9]	0.33[−9]	0.45[−9]	0.56[−9]	0.65[−9]	0.79[−9]	0.89[−9]	0.10[−8]	0.11[−8]
From $4p_{3/2}$ to $3d^{10}4s^2$		0.28[−10]	0.63[−10]	0.10[−9]	0.14[−9]	0.17[−9]	0.19[−9]	0.24[−9]	0.27[−9]	0.30[−9]	0.33[−9]
$4s4p_{1/2}$	[J=0]	0.52[−11]	0.12[−10]	0.18[−10]	0.24[−10]	0.29[−10]	0.34[−10]	0.40[−10]	0.45[−10]	0.49[−10]	0.52[−10]
$4s4p_{1/2}$	[J=1]	0.16[−10]	0.36[−10]	0.58[−10]	0.78[−10]	0.95[−10]	0.11[−9]	0.13[−9]	0.15[−9]	0.17[−9]	0.18[−9]
$4s4p_{3/2}$	[J=1]	0.61[−11]	0.15[−10]	0.26[−10]	0.37[−10]	0.46[−10]	0.55[−10]	0.69[−10]	0.79[−10]	0.92[−10]	0.10[−9]
$4s4p_{3/2}$	[J=2]	0.24[−10]	0.57[−10]	0.93[−10]	0.13[−9]	0.16[−9]	0.19[−9]	0.23[−9]	0.26[−9]	0.29[−9]	0.32[−9]
Total via $3d^9 4s^2 4p4d$		0.44[−10]	0.95[−10]	0.15[−9]	0.19[−9]	0.23[−9]	0.26[−9]	0.31[−9]	0.33[−9]	0.36[−9]	0.36[−9]
Total via $3d^9 4s^2 4p4f$		0.40[−10]	0.10[−9]	0.17[−9]	0.24[−9]	0.31[−9]	0.37[−9]	0.46[−9]	0.53[−9]	0.63[−9]	0.71[−9]
Total rate[a]		0.84[−10]	0.19[−9]	0.32[−9]	0.44[−9]	0.54[−9]	0.63[−9]	0.77[−9]	0.87[−9]	0.99[−9]	0.11[−8]

(c) Xe^{23+} (χ=716 eV)

	T_e/χ	0.3	0.4	0.5	0.6	0.7	0.8	1.0	1.2	1.6	2.0
Direct ionization											
$4p$		0.19[−11]	0.50[−11]	0.92[−11]	0.14[−10]	0.18[−10]	0.23[−10]	0.31[−10]	0.38[−10]	0.48[−10]	0.55[−10]
$4s$		0.24[−11]	0.71[−11]	0.12[−10]	0.19[−10]	0.26[−10]	0.33[−10]	0.45[−10]	0.57[−10]	0.76[−10]	0.90[−10]
$3d$		0.19[−12]	0.12[−11]	0.36[−11]	0.82[−11]	0.14[−10]	0.22[−10]	0.40[−10]	0.62[−10]	0.11[−9]	0.16[−9]
Total rate		0.45[−11]	0.13[−10]	0.25[−10]	0.41[−10]	0.58[−10]	0.78[−10]	0.12[−9]	0.16[−9]	0.24[−9]	0.31[−9]
Excitation-autoionization process											
From $4p_{1/2}$ to $3d^{10}4s^2$		0.16[−10]	0.36[−10]	0.59[−10]	0.80[−10]	0.10[−9]	0.12[−9]	0.15[−9]	0.17[−9]	0.20[−9]	0.21[−9]
$4s4p_{1/2}$	[J=0]	0.51[−11]	0.12[−10]	0.19[−10]	0.26[−10]	0.32[−10]	0.38[−10]	0.47[−10]	0.53[−10]	0.63[−10]	0.69[−10]
$4s4p_{1/2}$	[J=1]	0.12[−10]	0.28[−10]	0.45[−10]	0.62[−10]	0.77[−10]	0.90[−10]	0.11[−9]	0.13[−9]	0.15[−9]	0.16[−9]
$4s4p_{3/2}$	[J=1]	0.25[−11]	0.56[−11]	0.91[−11]	0.13[−10]	0.16[−10]	0.19[−10]	0.23[−10]	0.26[−10]	0.31[−10]	0.34[−10]
$4s4p_{3/2}$	[J=2]	0.14[−11]	0.32[−11]	0.52[−11]	0.70[−11]	0.87[−11]	0.10[−10]	0.12[−10]	0.14[−10]	0.16[−10]	0.17[−10]
Total via $3d^9 4s^2 4p4d$		0.29[−11]	0.59[−11]	0.87[−11]	0.11[−10]	0.13[−10]	0.15[−10]	0.17[−10]	0.19[−10]	0.20[−10]	0.20[−10]
Total via $3d^9 4s^2 4p4f$		0.34[−10]	0.79[−10]	0.13[−9]	0.18[−9]	0.22[−9]	0.26[−9]	0.32[−9]	0.37[−9]	0.43[−9]	0.48[−9]
Total rate[a]		0.37[−10]	0.84[−10]	0.14[−9]	0.19[−9]	0.23[−9]	0.27[−9]	0.34[−9]	0.38[−9]	0.45[−9]	0.50[−9]
From $4p_{3/2}$ to $3d^{10}4s^2$		0.29[−10]	0.61[−10]	0.94[−10]	0.12[−9]	0.15[−9]	0.17[−9]	0.21[−9]	0.23[−9]	0.26[−9]	0.28[−9]
$4s4p_{1/2}$	[J=0]	0.15[−11]	0.33[−11]	0.54[−11]	0.75[−11]	0.94[−11]	0.11[−10]	0.14[−10]	0.16[−10]	0.19[−10]	0.21[−10]
$4s4p_{1/2}$	[J=1]	0.45[−11]	0.10[−10]	0.17[−10]	0.23[−10]	0.29[−10]	0.35[−10]	0.43[−10]	0.49[−10]	0.58[−10]	0.65[−10]
$4s4p_{3/2}$	[J=1]	0.59[−11]	0.13[−10]	0.22[−10]	0.30[−10]	0.37[−10]	0.44[−10]	0.54[−10]	0.62[−10]	0.72[−10]	0.80[−10]

TABLE I. (*Continued*).

(c) Xe^{23+} (χ=716 eV)

	T_e/χ	0.3	0.4	0.5	0.6	0.7	0.8	1.0	1.2	1.6	2.0
$4sp4p_{3/2}$	[J=2]	0.11[−10]	0.24[−10]	0.39[−10]	0.54[−10]	0.67[−10]	0.79[−10]	0.97[−10]	0.11[−9]	0.13[−9]	0.14[−9]
Total via $3d^94s^24p4d$		0.17[−10]	0.35[−10]	0.51[−10]	0.66[−10]	0.77[−10]	0.86[−10]	0.99[−10]	0.11[−9]	0.11[−9]	0.11[−9]
Total via $3d^94s^24p4f$		0.34[−10]	0.77[−10]	0.12[−9]	0.17[−9]	0.22[−9]	0.25[−9]	0.32[−9]	0.36[−9]	0.42[−9]	0.47[−9]
Total rate[a]		0.51[−10]	0.11[−9]	0.18[−9]	0.24[−9]	0.29[−9]	0.34[−9]	0.42[−9]	0.47[−9]	0.54[−9]	0.59[−9]

(d) Pr^{28+} (χ=997 eV)

	T_e/χ	0.3	0.4	0.5	0.6	0.7	0.8	1.0	1.2	1.6	2.0
Direct ionization											
$4p$		0.12[−11]	0.31[−11]	0.55[−11]	0.83[−11]	0.11[−10]	0.14[−10]	0.18[−10]	0.22[−10]	0.28[−10]	0.32[−10]
$4s$		0.15[−11]	0.41[−11]	0.77[−11]	0.12[−10]	0.16[−10]	0.20[−10]	0.28[−10]	0.34[−10]	0.47[−10]	0.55[−10]
$3d$		0.13[−12]	0.79[−12]	0.23[−11]	0.53[−11]	0.89[−11]	0.14[−10]	0.25[−10]	0.39[−10]	0.69[−10]	0.95[−10]
Total rate		0.28[−11]	0.80[−11]	0.16[−10]	0.26[−10]	0.36[−10]	0.48[−10]	0.71[−10]	0.95[−10]	0.14[−9]	0.18[−9]
Excitation-autoionization process											
From $4p_{1/2}$ to $3d^{10}4s^2$		0.17[−10]	0.36[−10]	0.56[−10]	0.75[−10]	0.92[−10]	0.11[−9]	0.13[−9]	0.15[−9]	0.17[−9]	0.18[−9]
$4s4p_{1/2}$	[J=0]	0.62[−11]	0.14[−10]	0.21[−10]	0.29[−10]	0.36[−10]	0.42[−10]	0.52[−10]	0.59[−10]	0.69[−10]	0.76[−10]
$4s4p_{1/2}$	[J=1]	0.18[−11]	0.37[−11]	0.57[−11]	0.75[−11]	0.91[−11]	0.10[−10]	0.12[−10]	0.13[−10]	0.15[−10]	0.15[−10]
$4s4p_{3/2}$	[J=2]	0.15[−12]	0.32[−12]	0.51[−12]	0.69[−12]	0.84[−12]	0.98[−12]	0.12[−11]	0.13[−11]	0.15[−11]	0.17[−11]
$4s4p_{3/2}$	[J=1]	0.27[−13]	0.59[−13]	0.93[−13]	0.13[−12]	0.16[−12]	0.18[−12]	0.22[−12]	0.25[−12]	0.29[−12]	0.31[−12]
Total via $3d^94s^24p4f$		0.25[−10]	0.53[−10]	0.84[−10]	0.11[−9]	0.14[−9]	0.16[−9]	0.20[−9]	0.22[−9]	0.25[−9]	0.28[−9]
Total rate		0.25[−10]	0.53[−10]	0.84[−10]	0.11[−9]	0.14[−9]	0.16[−9]	0.20[−9]	0.22[−9]	0.25[−9]	0.28[−9]
From $4p_{3/2}$ to $3d^{10}4s^2$		0.11[−10]	0.24[−10]	0.38[−10]	0.51[−10]	0.63[−10]	0.73[−10]	0.88[−10]	0.99[−10]	0.12[−9]	0.13[−9]
$4s4p_{1/2}$	[J=0]	0.15[−11]	0.33[−11]	0.53[−11]	0.72[−11]	0.88[−11]	0.10[−10]	0.13[−10]	0.14[−10]	0.17[−10]	0.18[−10]
$4sp4p_{1/2}$	[J=1]	0.48[−11]	0.10[−10]	0.16[−10]	0.22[−10]	0.27[−10]	0.31[−10]	0.38[−10]	0.43[−10]	0.49[−10]	0.54[−10]
$4s4p_{3/2}$	[J=2]	0.72[−11]	0.16[−10]	0.25[−10]	0.33[−10]	0.41[−10]	0.48[−10]	0.58[−10]	0.66[−10]	0.76[−10]	0.83[−10]
$4s4p_{3/2}$	[J=1]	0.42[−12]	0.89[−12]	0.14[−11]	0.18[−11]	0.22[−11]	0.25[−11]	0.30[−11]	0.33[−11]	0.37[−11]	0.40[−11]
Total via $3d^94s^24p4f$		0.25[−10]	0.54[−10]	0.85[−10]	0.12[−9]	0.14[−9]	0.16[−9]	0.20[−9]	0.23[−9]	0.26[−9]	0.29[−9]
Total rate		0.25[−10]	0.54[−10]	0.85[−10]	0.12[−9]	0.14[−9]	0.16[−9]	0.20[−9]	0.23[−9]	0.26[−9]	0.29[−9]

(e) Eu^{32+} (χ=1254 eV)

	T_e/χ	0.3	0.4	0.5	0.6	0.7	0.81	1.0	1.2	1.6	2.0
Direct ionization											
$4s$		0.81[−12]	0.21[−11]	0.38[−11]	0.58[−11]	0.76[−11]	0.94[−11]	0.13[−10]	0.16[−10]	0.20[−10]	0.23[−10]
$4p$		0.15[−11]	0.38[−11]	0.73[−11]	0.10[−10]	0.14[−10]	0.17[−10]	0.23[−10]	0.28[−10]	0.37[−10]	0.43[−10]
$3d$		0.91[−13]	0.56[−12]	0.16[−11]	0.38[−11]	0.63[−11]	0.99[−11]	0.18[−10]	0.28[−10]	0.49[−10]	0.69[−10]
Total rate		0.24[−11]	0.65[−11]	0.13[−10]	0.20[−10]	0.28[−10]	0.36[−10]	0.54[−10]	0.72[−10]	0.11[−9]	0.13[−9]
Excitation-autoionization process											
From $4p_{1/2}$ to $3d^{10}4s^2$		0.14[−10]	0.30[−10]	0.47[−10]	0.62[−10]	0.75[−10]	0.86[−10]	0.10[−9]	0.11[−9]	0.13[−9]	0.14[−9]

TABLE I. (*Continued*).

(e) Eu^{32+} (χ=1254 eV)

	T_e/χ	0.3	0.4	0.5	0.6	0.7	0.81	1.0	1.2	1.6	2.0
$4s4p_{1/2}$	$[J=0]$	0.42[−13]	0.89[−13]	0.14[−12]	0.19[−12]	0.23[−12]	0.27[−12]	0.33[−12]	0.38[−12]	0.45[−12]	0.49[−12]
$4s4p_{1/2}$	$[J=1]$	0.13[−12]	0.28[−12]	0.43[−12]	0.59[−12]	0.73[−12]	0.85[−12]	0.10[−11]	0.12[−11]	0.14[−11]	0.15[−11]
$4s4p_{3/2}$	$[J=2]$	0.15[−14]	0.31[−14]	0.48[−14]	0.63[−14]	0.77[−14]	0.89[−14]	0.11[−13]	0.13[−13]	0.16[−13]	0.20[−13]
Total via $3d^9 4s^2 4p4f$		0.15[−10]	0.31[−10]	0.47[−10]	0.62[−10]	0.76[−10]	0.87[−10]	0.10[−9]	0.12[−9]	0.13[−9]	0.14[−9]
Total rate		0.15[−10]	0.31[−10]	0.47[−10]	0.62[−10]	0.76[−10]	0.87[−10]	0.10[−9]	0.12[−9]	0.13[−9]	0.14[−9]
From $4p_{3/2}$ to $3d^{10}4s^2$		0.11[−10]	0.24[−10]	0.37[−10]	0.49[−10]	0.59[−10]	0.68[−10]	0.81[−10]	0.90[−10]	0.10[−9]	0.11[−9]
$4s4p_{1/2}$	$[J=0]$	0.80[−12]	0.17[−11]	0.27[−11]	0.36[−11]	0.44[−11]	0.51[−11]	0.63[−11]	0.71[−11]	0.83[−11]	0.91[−11]
$4s4p_{1/2}$	$[J=1]$	0.18[−11]	0.37[−11]	0.58[−11]	0.78[−11]	0.95[−11]	0.11[−10]	0.13[−10]	0.15[−10]	0.17[−10]	0.19[−10]
$4s4p_{3/2}$	$[J=2]$	0.55[−13]	0.12[−12]	0.18[−12]	0.24[−12]	0.30[−12]	0.34[−12]	0.42[−12]	0.46[−12]	0.54[−12]	0.58[−12]
Total via $3d^9 4s^2 4p4f$		0.14[−10]	0.29[−10]	0.45[−10]	0.60[−10]	0.73[−10]	0.84[−10]	0.10[−9]	0.11[−9]	0.13[−9]	0.14[−9]
Total rate[a]		0.14[−10]	0.29[−10]	0.45[−10]	0.60[−10]	0.73[−10]	0.84[−10]	0.10[−9]	0.11[−9]	0.13[−9]	0.14[−9]

(f) Dy^{35+} (χ=1466.4 eV)

	T_e/χ	0.3	0.4	0.5	0.6	0.7	0.8	1.0	1.2	1.6	2.0
Direct ionization											
$4p$		0.66[−12]	0.17[−11]	0.31[−11]	0.46[−11]	0.60[−11]	0.74[−11]	0.10[−10]	0.12[−10]	0.15[−10]	0.18[−10]
$4s$		0.84[−12]	0.23[−11]	0.44[−11]	0.66[−11]	0.87[−11]	0.11[−10]	0.16[−10]	0.20[−10]	0.26[−10]	0.38[−10]
$3d$		0.78[−13]	0.47[−12]	0.14[−11]	0.31[−11]	0.51[−11]	0.80[−11]	0.14[−10]	0.22[−10]	0.38[−10]	0.53[−10]
Total rate		0.16[−11]	0.45[−11]	0.89[−11]	0.15[−10]	0.20[−10]	0.27[−10]	0.40[−10]	0.54[−10]	0.80[−10]	0.11[−9]
Excitation-autoionization process											
From $4p_{1/2}$ to $3d^{10}4s^2$		0.16[−11]	0.32[−11]	0.48[−11]	0.61[−11]	0.72[−11]	0.81[−11]	0.94[−11]	0.10[−10]	0.12[−10]	0.14[−10]
$4s4p_{1/2}$	$[J=0]$	0.82[−15]	0.17[−14]	0.27[−14]	0.37[−14]	0.46[−14]	0.53[−14]	0.66[−14]	0.75[−14]	0.88[−14]	0.96[−14]
$4s4p_{1/2}$	$[J=1]$	0.22[−14]	0.46[−14]	0.72[−14]	0.98[−14]	0.12[−13]	0.14[−13]	0.18[−13]	0.20[−13]	0.24[−13]	0.26[−13]
Total via $3d^9 4s^2 4p4f$		0.16[−11]	0.32[−11]	0.48[−11]	0.61[−11]	0.73[−11]	0.82[−11]	0.94[−11]	0.10[−10]	0.12[−10]	0.14[−10]
Total rate		0.16[−11]	0.32[−11]	0.48[−11]	0.61[−11]	0.73[−11]	0.82[−11]	0.94[−11]	0.10[−10]	0.12[−10]	0.14[−10]
From $4p_{3/2}$ to $3d^{10}4s^2$		0.11[−10]	0.23[−10]	0.35[−10]	0.45[−10]	0.54[−10]	0.62[−10]	0.75[−10]	0.83[−10]	0.10[−9]	0.12[−9]
$4s4p_{1/2}$	$[J=0]$	0.61[−14]	0.12[−13]	0.16[−13]	0.20[−13]	0.23[−13]	0.25[−13]	0.26[−13]	0.27[−13]	0.29[−13]	0.34[−13]
$4s4p_{1/2}$	$[J=1]$	0.82[−14]	0.17[−13]	0.25[−13]	0.32[−13]	0.38[−13]	0.43[−13]	0.51[−13]	0.56[−13]	0.64[−13]	0.71[−13]
Total via $3d^9 4s^2 4p4f$		0.11[−10]	0.23[−10]	0.35[−10]	0.45[−10]	0.55[−10]	0.62[−10]	0.75[−10]	0.84[−10]	0.10[−9]	0.12[−9]
Total rate		0.11[−10]	0.23[−10]	0.35[−10]	0.45[−10]	0.55[−10]	0.62[−10]	0.75[−10]	0.84[−10]	0.10[−9]	0.12[−9]

[a]Including transitions to $3d^{10}4s4d$ and $3d^{10}4p^2$ configurations.

ground levels. Total EA rates are also reported, which include, in addition, transitions to $3d^{10}4s4d$ and $3d^{10}4p^2$ final configurations, when autoionization to these levels is possible. In order to show the contribution of each of the intermediate inner-shell excited configurations $3d^94s^24p4d$, $3d^94s^24p4f$, total EA rates via each configuration are also given separately.

For the lighter elements, the autoionizing levels involve both $3d^94s^24p4d$ and $3d^94s^24p4f$ configurations whereas, for the heavier elements, only the latter configuration is above the ionization threshold. This feature is illustrated by Fig. 1 where the average energy of the two inner-shell excited configurations in χ units is plotted as a function of Z. Taking into account the spread of the levels around these averages and the effect of configuration interactions, the result is a continuous crossing of the levels through the χ line as Z increases. In Mo^{11+}, both $3d^94s^24p4d$ and $3d^94s^24p4f$ are autoionizing and all the lower $3d^{10}4s^2$, $4s4p$, $4s4d$, and $4p^2$ levels of the Zn I–like ion can be populated through this process. Whereas for Dy^{35+} only some of the $3d^94s^24p4f$ levels are autoionizing and only the ground state $3d^{10}4s^2$ of Dy^{36+} may be populated by this process. This continuous change of the relative position of the ionization potential and the inner-shell excited levels is at the origin of the peculiar trend of the EA rate along the Ga I–like isoelectronic sequence. A typical Z dependence of EA (from $4p_{1/2}$), DI, and their ratio R at $T_e=\chi$ are shown for Pr^{28+} in Fig. 2 [data taken from Table I(d)].

In the low-Z range (Mo), although the mean branching ratio for autoionization remains close to unity, the ratio R is reduced, due to the fact that the $4d$ and $4f$ inner-shell excited configurations are relatively high with respect to the first ionization limit, disadvantaging thus the excitation processes. On the other hand, for elements heavier than Xe, some levels of the inner-shell excited configurations become lower than the ionization limit and cease to contribute to EA processes.

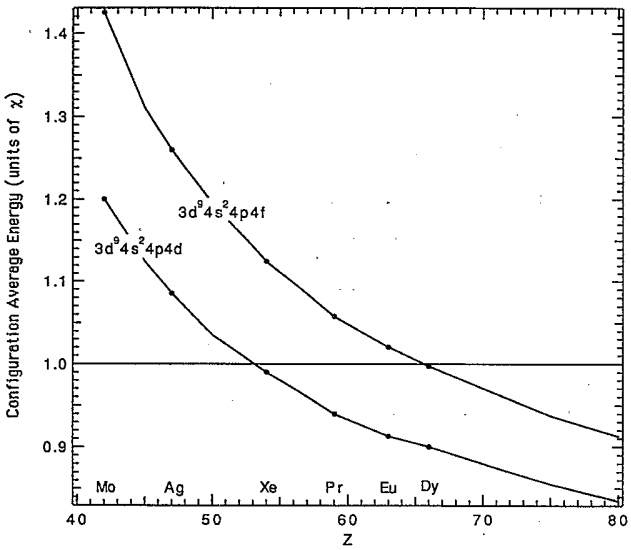

FIG. 1. Ratio of the average energies of the configurations $3d^94s^24p4d$ and $3d^94s^24p4f$ to the ionization potential $\chi(Z)$ as a function of Z.

TABLE II. Branching ratio B^C [Eq. (6)] for the excitation autoionization process, at $T_e=\chi$.

Initial level	$i=3d^{10}=4s^24p_{1/2}$		$i=3d^{10}4s^24p_{3/2}$	
Inner-shell excited configuration	$c=4d$	$c=4f$	$c=4d$	$c=4f$
Mo XII	0.99	0.98	0.98	0.99
Ag XVII	0.96	0.95	0.89	0.96
Xe XXIV	0.12	0.88	0.68	0.87
Pr XXIX	0.00	0.69	0.00	0.70
Eu XXXIII	0.00	0.47	0.00	0.45
Dy XXXVI	0.00	0.05	0.00	0.37

To illustrate a temperature-independent change of the EA rate along the isoelectronic sequence, the following procedure has been used: A branching ratio to autoionization has been calculated for the $3d$-$4d$ and $3d$-$4f$ transitions and separately for the $i=3d^{10}4s^24p_{1/2}$, $3d^{10}4s^24p_{3/2}$ initial levels. For each involved inner-shell excited configuration $C=3d^94s^24p4d$, $3d^94s^24p4f$ separately these branching ratios are obtained from the ratio of the EA to total excitation rate:

$$B^C \equiv \left[\frac{\sum_k X_{ik}^C}{\sum_{j\in C} Q_{ij}} \right], \tag{6}$$

where

$$X_{ik}^C \equiv \sum_{j\in C} Q_{ij} \left[\frac{A_{jk}^a}{\sum_l A_{jl}^a + \sum_m A_{jm}} \right]. \tag{7}$$

These ratios are almost independent of the electron temperature in the range involved. In Table II these average branching ratios are given as function of the Z of the element and at a temperature equal to the ionization potential of the ion, although it is very insensitive to tempera-

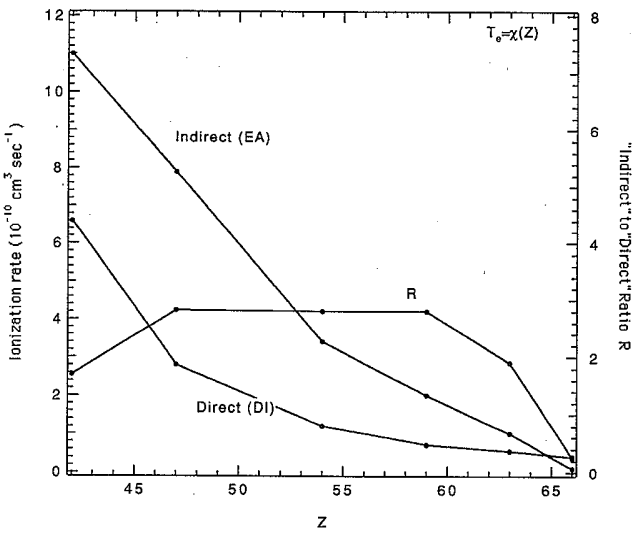

FIG. 2. Indirect ionization rate (EA from the ground state $4p_{1/2}$), direct ionization rate, and ratio R as functions of Z.

ture change. As the excited levels cross the ionization potenial χ line, the branching ratio for the autionization falls. This occurs first for those levels excited from the $3d^{10}4s^24p_{1/2}$ which are lower than those excited from $3d^{10}4s^24p_{3/2}$. This effect is far more important than the lowering of the branching ratio due to the increasing importance of radiative decay with Z.

B. Temperature dependence

Comparison in Table I of the EA process through $\Delta n = 1$ transitions with direct ionization rates (including inner shell) shows that for the lower part of the isoelectronic sequence the EA process is dominant at electronic temperature lower than the ionization potential. Figure 3 displays a typical result of the dependence of the ratio of EA (from $4p_{1/2}$) to direct ionization. The general trend of the ratio curve R can be understood following the procedure used by Cowan and Mann [3]. Indeed, assuming that only outer electrons contribute to the direct ionization rates (i.e., $4s$, $4p$ but not $3d$), which is true at relatively low electron temperature, and since the ionization potential of $4s$ and $4p$ electrons are very close, it can be shown that this curve should have a maximum for an electron temperature close to the difference between the energy of the autoionizing levels and the ionization potential χ. In the Ga-like case the maximum occurs at very low temperature and thus is not seen in Fig. 3. This difference is very small, changing from 87 eV in Mo XII to 10 eV in Dy XXXVI (for the $3d$-$4f$ excitation). In any case such electron temperature is much lower than the Ga I–like temperature of most abundance at coronal conditions. This differs from the situation in the Na I–like sequence, where the difference is generally greater than the electron temperature of most abundance [3]. This explains the fact that for the Ga-like sequence the ratio of EA to direct ionization DI is a decreasing function of the electronic temperature in the relevant temperature range (at high temperature this decreasing is even more accentuated, due to the increasing contribution of the ten $3d$ electrons to direct ionization). The relative importance of EA compared to direct ionization is thus determined by the value of this ratio around the Ga-like temperature of most abundance at coronal equilibrium conditions.

IV. DENSITY-DEPENDENT IONIZATION RATE

In the case of dysprosium, calculations give a significant difference between the EA rates calculated from the $4p_{1/2}$ and $4p_{3/2}$ levels [see Table I(f)]. The difference comes from the fact that essentially only $3d^94s^24p_{3/2}4f$ levels (which are collisionally excited from $4p_{3/2}$ only) lie above the ionization limit χ.

This gives a density-dependent EA rate; indeed, at low densities ($n_e < 10^{16}$ cm^{-3}) [4], the $4p_{3/2}$ level is not populated because of the magnetic dipole decay from $4p_{3/2}$ to $4p_{1/2}$. In this case the EA rate is negligible in comparison with the direct ionization rate. At higher densities, however, because of the electron impact excitation and deexcitation, these levels are populated according to their statistical weight, and the EA rate is no more negligible. Density-dependent ionization rate has already been observed in some other isoelectronic sequences, for example, in Be I–like ions [9]. In Ga I–like case, this interesting feature should be expected not only for the Dy XXXVI ions, but also for the neighboring ions of the isoelectronic sequence.

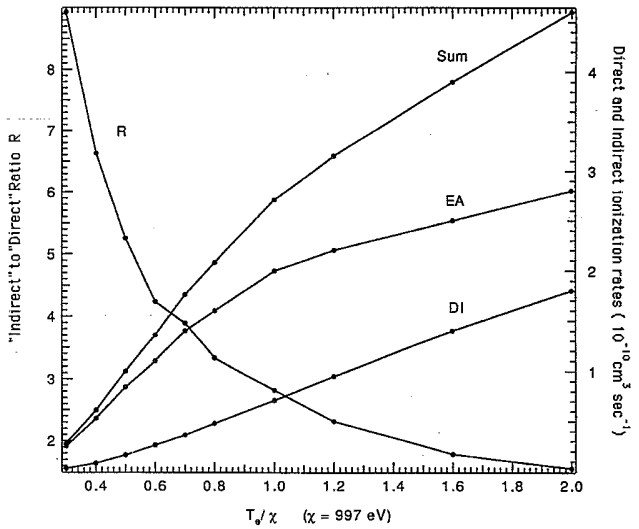

FIG. 3. Indirect ionization rate (EA from the ground state $4p_{1/2}$) and direct ionization rate, their ratio and sum, as functions of the electronic temperature for Pr XXIX.

V. CONCLUSION

In the present work results of the computations for direct ionization and excitation-ionization rates through $\Delta n = 1$ inner-shell excitations have been presented for six ions along the Ga I–like isoelectronic sequence. It was shown that EA processes are the dominant ionizing mechanisms for highly ionized Ga I–like elements up to Eu, in intermediate temperature range. These processes should thus be taken into account in ionization equilibrium models. Moreover, the peculiar trend to EA processes along the Ga I isoelectronic sequence has been studied. Crossing of the inner-shell excited levels with the ionization limit while the Z of the element increases along the sequence, causes a drastic change of the EA rates. Finally, an interesting density dependence of the effective ionization rates for elements around Dy has been predicted.

*Permanent address: The Nuclear Research Center of the Negev, P.O. Box 9001, Beer Sheva, Israel.

[1] J. W. Allen and A. K. Dupree, Astrophys. J. **155**, 27 (1969).

[2] D. C. Griffin, M. S. Pindzola, and C. Bottcher, Phys. Rev. A **36**, 3642 (1987).

[3] R. D. Cowan and J. B. Mann, Astrophys. J. **232**, 940 (1979).

[4] P. Mandelbaum, M. Finkenthal, E. Meroz, J. L. Schwob, J. Oreg, W. H. Goldstein, M. Klapisch, A. L. Osterheld,

A. Bar-Shalom S. Lippman, L. K. Huang, and H. W. Moos, Phys. Rev. A **42**, 4412 (1990).

[5] L. A. Vainshtein, L. P. Presnyakov, and I. I. Sobelman, Zh. Eksp. Theor. Fiz. **45**, 2015 (1963) [Sov. Phys.—JETP **18**, 1383 (1964)].

[6] M. Klapisch, J. L. Schwob, B. S. Fraenkel, and J. Oreg, J. Opt. Soc. Am. **61**, 148 (1977).

[7] A. Bar-Shalom, M. Klapisch, and J. Oreg, Phys. Rev. A **38**, 1773 (1988).

[8] J. Oreg, W. H. Goldstein, M. Klapisch, and A. Bar-Shalom, following paper, Phys. Rev. A **44**, 1750 (1991).

[9] J. E. Vernazza and J. C. Raymond, Astrophys. J. **228**, L89 (1979).